

# F- and G-type stars with planetary companions: $\nu$ Andromedae, $\rho^1$ Cancri, $\tau$ Bootis, 16 Cygni and $\rho$ Coronae Borealis\*

Klaus Fuhrmann, Michael J. Pfeiffer, and Jan Bernkopf

Institut für Astronomie und Astrophysik der Universität München, Scheinerstraße 1, D-81679 München, Germany

Received 25 March 1998 / Accepted 15 April 1998

**Abstract.** Accurate stellar parameters are presented for the F- and G-type stars  $\nu$  And,  $\rho^1$  Cnc,  $\tau$  Boo, 16 Cyg, and  $\rho$  CrB, which are deemed to possess planetary companions from intense Doppler monitoring. Evolutionary tracks that employ detailed model atmospheres as upper boundary condition and allow for helium diffusion are computed for the individual stars to derive the stellar masses and ages. From a comparison of the spectroscopic parallaxes with the accurate distances available from the Hipparcos satellite well-defined constraints on the stellar surface gravities are obtained in good agreement with our spectroscopically deduced values.

**Key words:** stars: distances – stars: evolution – stars: fundamental parameters – stars: planetary systems

## 1. Introduction

On the heels of objects such as 51 Peg, HD 114762 and Gliese 229, the list of sub-stellar companions around ordinary stars is steadily increasing. Some of them are regarded as planets, others as brown dwarfs. Due to the usually unknown orbital inclination, which causes the derived companion masses to represent only lower limits, a certain classification is not always possible. As a result, some planetary candidates may instead belong to the realm of brown dwarfs. Likewise, a number of putative brown dwarfs might actually be low-mass stars.

The present investigation is an attendant contribution to our recent analysis of the solar-type stars 51 Peg and 47 UMa (Fuhrmann, Pfeiffer & Bernkopf 1997). It concentrates on the *stellar* component of only those systems, where the low-mass companions are considered to be planets.

We analyze the 51 Peg-type systems  $\nu$  Andromedae (F8V),  $\rho^1$  Cancri (G8V) and  $\tau$  Bootis (F7V), detected as such by Butler et al. (1997). Next, we consider 16 Cygni, actually a triple star system (two solar-type components A+B and a distant M dwarf), where the B component has been announced by Cochran et al. (1996) to exhibit a Jupiter mass companion in a highly eccentric orbit. The planet's large orbital eccentricity may be the result of gravitational interactions with 16 Cyg A (e.g. Cochran

et al. 1997), displaced at a projected separation of  $\sim 840$  AU, which we therefore include in the analysis. Finally, we investigate  $\rho$  Coronae Borealis – a slightly metal-poor turnoff star – around which a 51 Peg-type planet has been found by Noyes et al. (1997).

For similar recent analyses such as ours, we draw attention to the work of Gonzalez (1997, 1998), who has treated the complete sample of the parent stars of extrasolar planetary system candidates, and to the analysis of 51 Peg by Tomkin et al. (1997).

## 2. Observations

Most of the observations were carried out in May 1997 with the 2.2m telescope at the Calar Alto Observatory. The recently installed fiber-coupled Cassegrain échelle spectrograph FOCES (Pfeiffer et al. 1998) was employed along with a  $2048^2$   $15\mu$  CCD at a resolution of  $\lambda/\Delta\lambda \sim 60000$ . The spectral range covers 3800–9200Å with short gaps only longward of  $\sim 8800\text{Å}$ . One object,  $\nu$  And, could not be observed in May 1997, but incidentally this was done in the context of another program in September 1996, albeit with a  $1024^2$   $24\mu$  CCD and consequently at a somewhat lower resolution of about  $\lambda/\Delta\lambda \sim 35000$ . All stars were observed at least twice and since all are bright objects, exposure times are short and signal-to-noise values high.

## 3. Stellar parameters

The spectroscopic analysis is done in a similar way as in our recent work on 51 Peg and 47 UMa: the Balmer lines  $H\alpha$  and  $H\beta$  are used to determine the effective temperature; the surface gravity is deduced from the iron ionization equilibrium, but requires systematic adjustments to higher values for the hotter members of our sample from a comparison of the wings of the Mg Ib lines. The iron abundance and microturbulence parameter are derived from line profile analyses and by forcing the results to be independent of equivalent widths. For this purpose the instrumental profile is deduced from additional spectra of the Moon in combination with the Kitt Peak Solar Flux Atlas (Kurucz et al. 1984). Values for the radial-tangential macroturbulence  $\zeta_{RT}$  are not determined from our spectra, since this parameter is known to possess compensatory characteristics with respect to the projected rotational velocity  $v\sin i$  and our data

\* Based on observations collected at the German Spanish Astronomical Center, Calar Alto, Spain

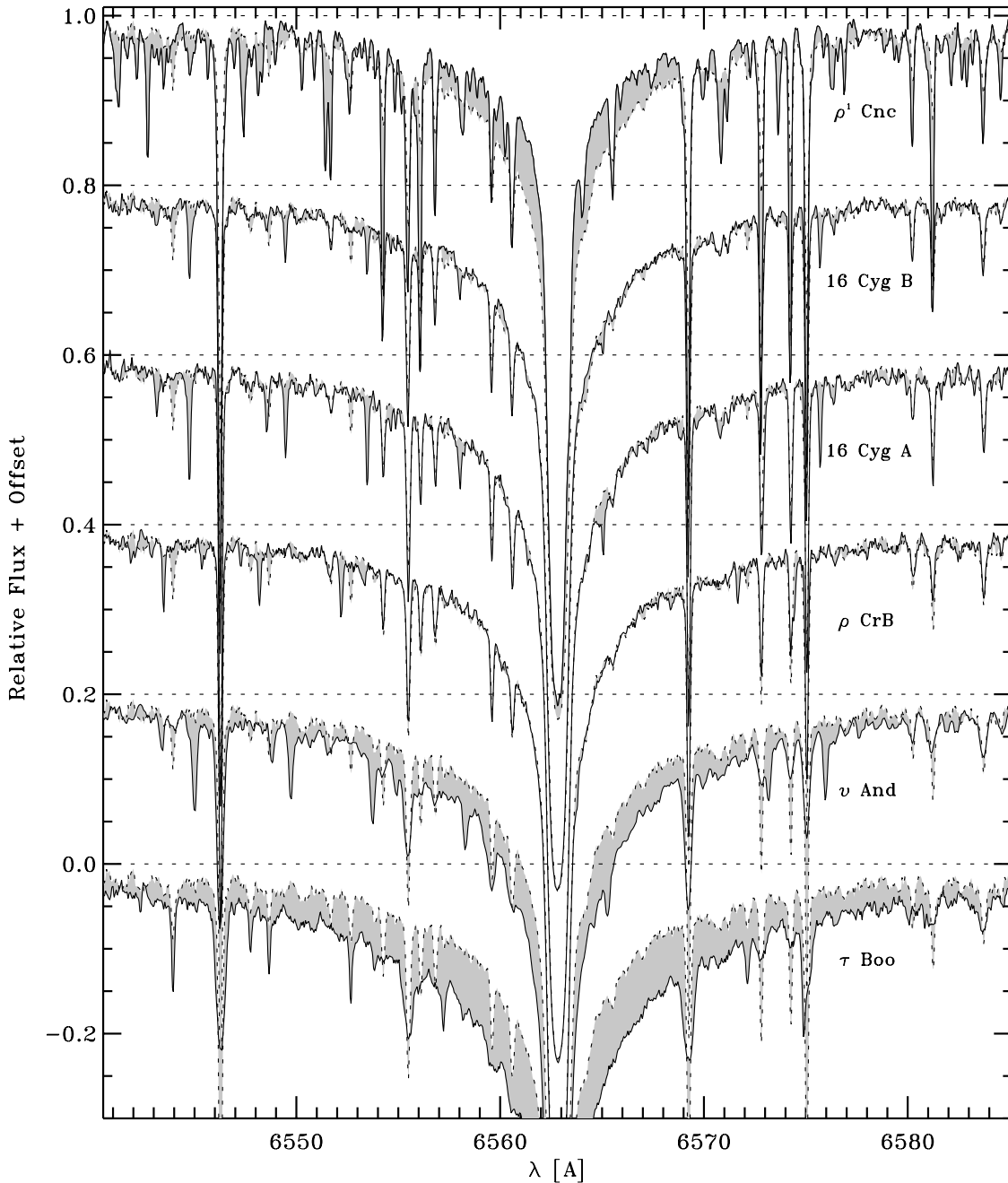


**Fig. 1.**  $H\alpha$  line profiles of  $\rho^1$  Cnc, 16 Cyg B, 16 Cyg A,  $\rho$  CrB,  $v$  And, and  $\tau$  Boo. This sequence of increasing effective temperatures (top to bottom) is superimposed by the spectrum of the Moon (dotted curve) with differences depicted by shading

are actually not as resolved as to put real constraints on either quantity. Instead, we use the relation

$$\zeta_{RT} \sim 3.95 \times 10^{-3} T_{eff}[\text{K}] - 19.25$$

given by Gray (1984), that is valid for main-sequence stars, and adopt slightly higher values for evolved stars (cf. Gray 1992, p.416). After having fixed the macroturbulence parameter this way, the  $v \sin i$  value is immediately obtained as the residual component to the absorption line profiles.

#### *v Andromedae*

This object is one of the bright standard F stars. Early spectroscopic investigations (Powell 1970, Spite & Spite 1973, Hearnshaw 1974) concur at  $[\text{Fe}/\text{H}] = -0.16$ , a value that enters many subsequent analyses (e.g. Carney 1979, Saxner & Hammarbäck 1985, Blackwell & Lynas-Gray 1994). More recent investigations however reveal a metallicity some 0.1 dex higher than solar.

Our effective temperature determination from the wings of  $H\alpha$  (displayed in Fig. 1) and  $H\beta$  results in  $T_{eff} = 6107 \pm 80$  K.

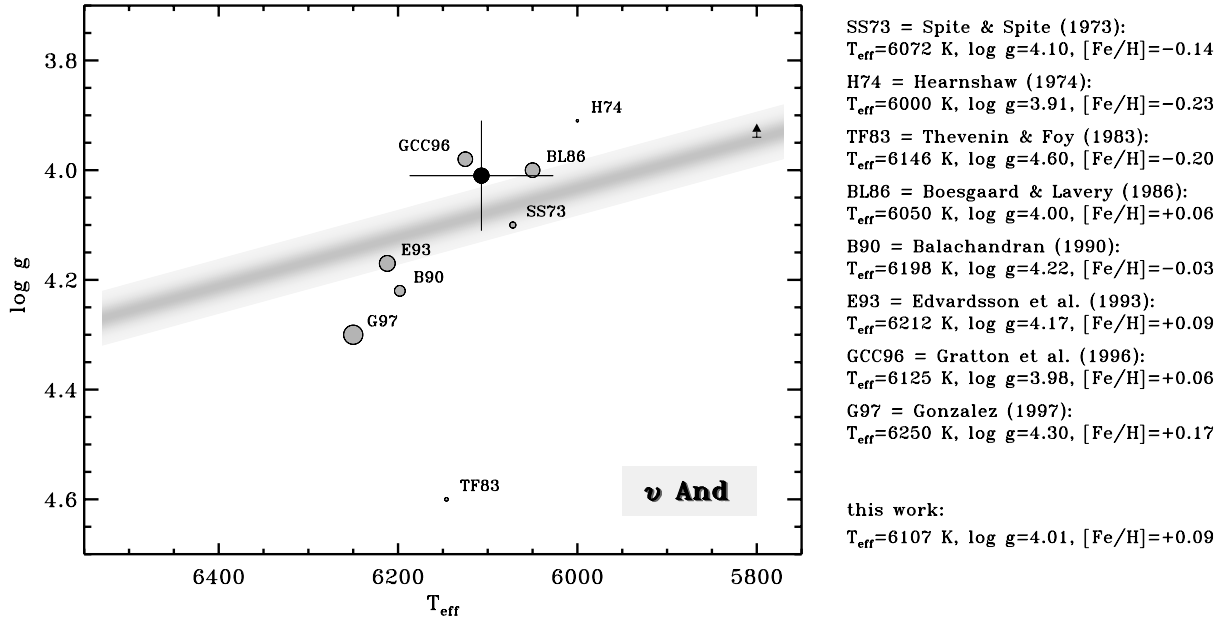


**Fig. 2.** The HR diagram for  $\nu$  And. The black dot marks our spectroscopically derived value for the effective temperature and surface gravity with error bars included. The upwards tilted grayscale bar displays the most probable  $T_{\text{eff}}\text{-log } g$  parameter space for this star, as essentially prescribed by the accurate Hipparcos distance scale. The small circles represent comparisons to previous work from the literature, with diameters in proportion to the derived metallicity. A systematic shift of the bar as a result of deviating metallicity scales from different analyses is indicated by the vertical arrow for a decrease in  $[\text{Fe}/\text{H}]$  by 0.1 dex

For the surface gravity the Mg Ib lines imply  $\log g = 4.01 \pm 0.10$ , whereas a value  $\log g = 3.88$  would result from the iron ionization equilibrium method. The metallicity of  $\nu$  And from line profile analyses of Fe II lines is found to be  $[\text{Fe}/\text{H}] = +0.09 \pm 0.06$ , where the uncertainty denotes the  $2\sigma$  rms error.

In Fig. 2 this result is compared to other abundance analyses, most of which are found in the catalogue of  $[\text{Fe}/\text{H}]$  determinations of Cayrel de Strobel et al. (1997). For an easy assessment of the differences that exist in the literature we display all data in the  $T_{\text{eff}}\text{-log } g$  plane of the HR diagram as small circles, with circle diameters in proportion to the value of the metallicity. Explicit numbers and the references to the labels in Fig. 2 are given at the right side of the diagram. Our own abundance analysis is depicted by the black dot, along with the uncertainties in  $T_{\text{eff}}$  and  $\log g$  as mentioned above.

According to

$$\log \pi = 0.5([g] - [M]) - 2[T_{\text{eff}}] - 0.2(V + BC_V + 0.26)$$

(with  $M_{\text{bol},\odot}=4.74$  and the usual logarithmic notation  $[X] = \log(X/X_\odot)$ ) and with the accurate parallaxes from Hipparcos at our disposal, it is important to realize that every point in the  $T_{\text{eff}}\text{-log } g$  plane of Fig. 2 corresponds to a well-defined stellar mass. By means of the precise bolometric magnitudes from the Hipparcos astrometry and with values for  $T_{\text{eff}}$  and  $[\text{Fe}/\text{H}]$ , quite accurate stellar masses can however be derived. In other words, every  $T_{\text{eff}}$  value in Fig. 2 has a corresponding  $\log g$  value, whose accuracy is to a good approximation fixed by the stellar mass determination and entails the grayscale bar that delineates the most probable  $T_{\text{eff}}\text{-log } g$  parameter space for  $\nu$  And.

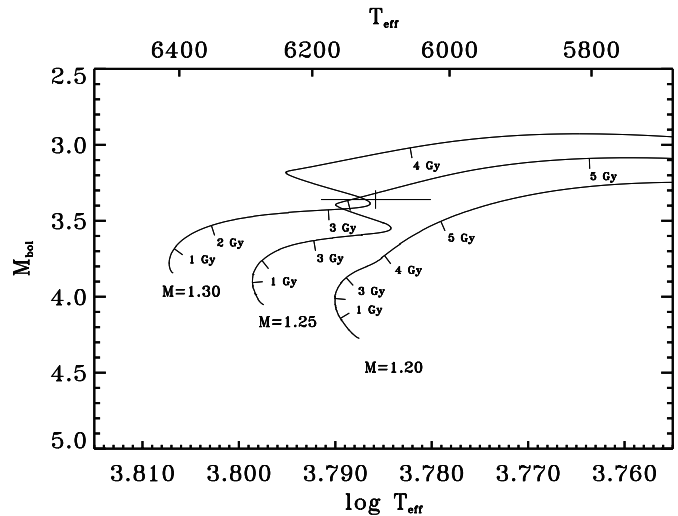


**Fig. 3.** Evolutionary tracks with  $M_* = 1.20, 1.25$  and  $1.30 M_\odot$  and a metallicity  $[\text{Fe}/\text{H}]=+0.09$ , as derived for  $\nu$  And. Tick marks are given in steps of 1 Gyr. The stellar mass and age are found to be  $1.27 \pm 0.06 M_\odot$  and  $3.8 \pm 1.0$  Gyr

In principle, additional uncertainties are also introduced from the expected errors of the visual magnitude and bolometric correction, but they are of only minor importance. Data for the latter are taken from Alonso, Arribas & Martínez-Roger (1995) and are generally small for all our sample stars. Comparison to the  $BC$ 's of Vandenberg & Bell (1985) reveal only small differences ( $\sim 0.03$  mag) and we adopt  $\Delta BC_V \simeq 0.05$  mag as a common representative error. The visual magnitudes and

**Table 1.** Stellar parameters of the program stars. Most of the entries are self-explanatory;  $d_{\text{HIP}}$  is the distance obtained from the Hipparcos satellite,  $d_{\text{sp}}$  the spectroscopically deduced value. For each star the second row indicates the error estimates, the macroturbulence value  $\zeta_{RT}$  is *adopted* according to the relations given in Gray (1984, 1992). For the sake of completeness, we also include the results of our companion paper on 51 Peg and 47 UMa, supplemented by minor updates

Object	HR	HD	$V$	$T_{\text{eff}}$ [K]	$\log g$	[Fe/H]	$\xi_t$ [km/s]	$\zeta_{RT}$ [km/s]	$v \sin i$ [km/s]	$M_V$	$M_{\text{bol}}$	$BC_V$	Mass [ $M_{\odot}$ ]	Radius [ $R_{\odot}$ ]	Age [Gyr]	$d_{\text{HIP}}$ [pc]	$d_{\text{sp}}$ [pc]
$\nu$ And	458	9826	4.086 0.013	6107 80	4.01 0.1	+0.09 0.06	1.40 0.20	5.4	9.5 0.8	3.44 0.02	3.36 0.06	-0.08 0.05	1.27 0.06	1.69 0.06	3.8 1.0	13.47 0.13	14.69 2.01
$\rho^1$ Cnc	3522	75732	5.942 0.015	5336 90	4.47 0.1	+0.40 0.07	0.76 0.20	1.9	2.5 1.0	5.45 0.03	5.23 0.06	-0.22 0.05	1.08 0.06	0.94 0.04	<5	12.53 0.13	13.45 1.87
$\tau$ Boo	5185	120136	4.496 0.008	6360 80	4.17 0.1	+0.27 0.08	1.56 0.20	6.3	15.6 0.7	3.53 0.03	3.48 0.06	-0.05 0.05	1.42 0.05	1.48 0.05	1.0 0.6	15.60 0.17	17.19 2.35
$\rho$ CrB	5968	143761	5.412 0.016	5821 80	4.12 0.1	-0.24 0.08	1.10 0.20	4.1	1.0 1.0	4.21 0.03	4.07 0.06	-0.14 0.05	0.97 0.05	1.34 0.05	10.2 1.7	17.43 0.22	18.47 2.54
16 Cyg A	7503	186408	5.960 0.009	5805 60	4.26 0.1	+0.06 0.05	1.03 0.20	3.9	2.0 1.0	4.28 0.03	4.16 0.06	-0.12 0.05	1.04 0.04	1.29 0.04	8.0 1.4	21.62 0.24	20.96 2.85
16 Cyg B	7504	186427	6.215 0.014	5766 60	4.29 0.1	+0.05 0.05	0.89 0.20	3.7	1.5 1.0	4.56 0.03	4.43 0.06	-0.13 0.05	1.01 0.04	1.16 0.04	8.0 1.8	21.41 0.24	22.08 3.01
47 UMa	4277	95128	5.051 0.016	5892 70	4.27 0.1	+0.00 0.07	1.01 0.20	4.0	1.5 1.0	4.31 0.03	4.19 0.06	-0.12 0.05	1.03 0.05	1.24 0.04	7.4 1.9	14.08 0.13	14.03 1.92
51 Peg	8729	217014	5.463 0.020	5793 70	4.33 0.1	+0.20 0.07	0.95 0.20	3.7	2.0 1.0	4.53 0.03	4.41 0.06	-0.12 0.05	1.11 0.06	1.16 0.04	4.0 2.5	15.36 0.18	15.85 2.17

corresponding error estimates are those given in Mermilliod, Mermilliod & Hauck (1997).

The mass and age of  $\nu$  And are calculated from evolutionary tracks that make use of model atmospheres as upper boundary condition (cf. Bernkopf 1998) and include helium diffusion. Fig. 3 displays the results valid for [Fe/H]=+0.09. Interestingly, the star resides in the hook-region that causes some uncertainty for its evolutionary stage. We adopt  $M_{\star} = 1.27 \pm 0.06 M_{\odot}$  and an age  $3.8 \pm 1.0$  Gyr, whereby the uncertainties denote the effects of the quadratic addition of  $\Delta M_{\text{bol}}$ ,  $\Delta T_{\text{eff}}$  and  $\Delta[\text{Fe}/\text{H}]$ .

Fig. 2 shows that we are slightly above the most probable  $T_{\text{eff}}\text{-}\log g$  parameter combination. A shift to *lower* effective temperatures lessens this deviation, but is not implied from a comparison with data of the infrared flux method: Blackwell & Lynas-Gray (1994) and Alonso, Arribas & Martínez-Roger (1996) get  $T_{\text{eff}} = 6205$  K and  $T_{\text{eff}} = 6155$  K, respectively. Instead, we rather presume that our value for the surface gravity determination may be too low by  $\sim 0.07$  dex, which is anyhow within the accuracy of the method.

Projected rotational velocities of  $\nu$  And from the literature concur at  $v \sin i \sim 9 \text{ km s}^{-1}$ : Soderblom (1982),  $v \sin i = 9.2 \pm 0.7 \text{ km s}^{-1}$ ; Benz & Mayor (1984),  $v \sin i = 9.3 \pm 0.4 \text{ km s}^{-1}$ ; Gray (1986),  $v \sin i = 9.0 \pm 0.4 \text{ km s}^{-1}$ ; Balachandran (1990),  $v \sin i = 8 \pm 3 \text{ km s}^{-1}$ ; and Gonzalez (1997),  $v \sin i = 9.0 \pm 0.5 \text{ km s}^{-1}$ . From our analysis we get  $v \sin i = 9.5 \pm 0.8 \text{ km s}^{-1}$ , in good agreement with the above mentioned results.

The radius of  $\nu$  And,  $R_{\star} = 1.69 \pm 0.06 R_{\odot}$ , is immediately obtained from  $M_{\text{bol}}$  and  $T_{\text{eff}}$ . The high accuracy benefits again from the precision of the Hipparcos astrometry. Along with the

rotational period of  $\sim 12.2$  days, derived from the Ca II activity parameter  $R'_{\text{HK}}$  (cf. Soderblom 1985), a high inclination angle is indicated.

In Table 1 all relevant data are summarized, which also include the astrometric and our spectroscopic distance values for  $\nu$  And.

### $\rho^1$ Cancri

$\rho^1$  Cnc reveals an extraordinary strong absorption line spectrum which is by no means the mere result of the late G-type, but also reflects a genuine overabundance of the stellar photosphere by approximately 0.4 dex above solar. This extreme metal content not only classifies  $\rho^1$  Cnc as a so-called super-metal-rich star, but is indeed at the high end for this category of stars in the solar neighborhood.

In this context it is quite remarkable that  $\rho^1$  Cnc has repeatedly been claimed to be as old as, or close to, the age of the Galaxy (cf. Perrin et al. 1977, Cayrel de Strobel 1987, Gonzalez 1998), a result that is somewhat in conflict with our notions of chemical evolution and will be addressed below.

Fig. 1 gives an illustration of the metal-rich line spectrum of  $\rho^1$  Cnc around H $\alpha$ , a region that normally displays only few, mostly telluric, absorption lines. In fact, the high metal content of  $\rho^1$  Cnc in combination with its comparatively late spectral type prevented us to include H $\beta$  for the effective temperature determination. Hence, the value given in Table 1,  $T_{\text{eff}} = 5336 \pm 90$  K, is based on only the H $\alpha$  spectra, both of which show however consistent results.

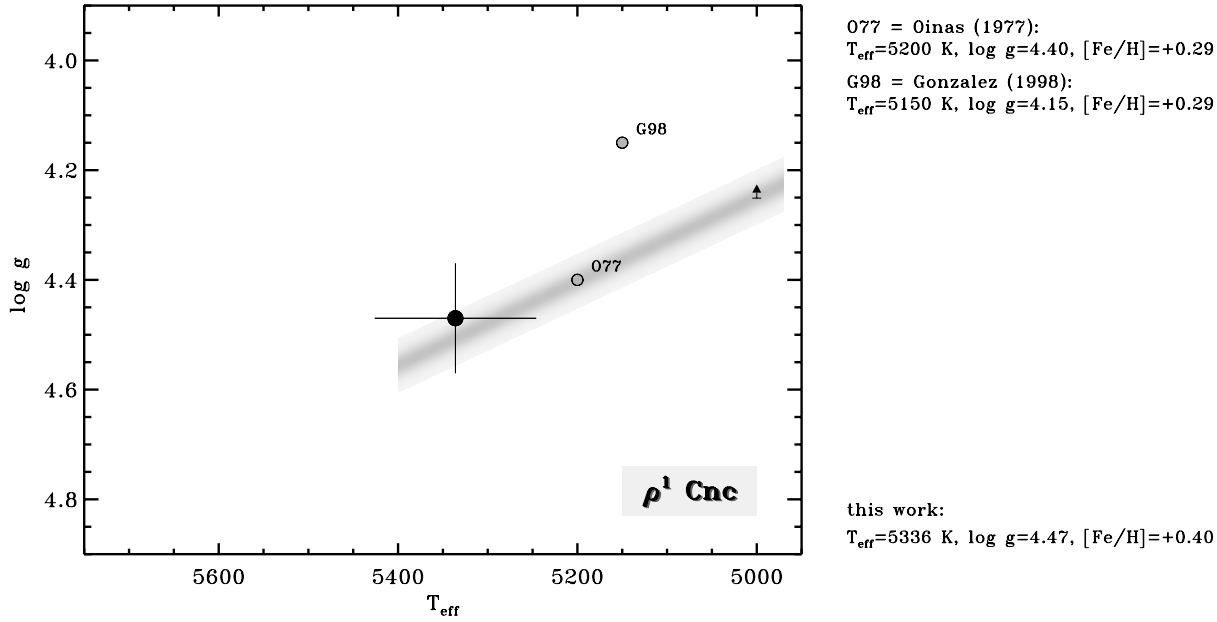


**Fig. 4.** Same as Fig. 2, but for  $\rho^1$  Cnc. Effective temperatures higher than  $\sim 5400$  K produce unrealistic positions below the main-sequence (cf. Fig. 5)

The surface gravity, if derived from the iron ionization equilibrium, is found to be  $\log g = 4.51$ . With reference to the Mg Ib lines this value is reduced to  $\log g = 4.47$ , which slightly improves the modeling of the observed strong line profiles. We note however that the mere decrease of  $\sim 20$  K for the effective temperature value corresponds to a  $\sim 0.04$  dex reduction in  $\log g$  if the latter is deduced from the iron ionization equilibrium. In other words, while it is important to verify the results of both  $\log g$  methods, there is no real discrepancy from either use in the spectra of  $\rho^1$  Cnc, although a peek at the  $T_{\text{eff}}\text{-}\log g$  Kiel diagram in Fig. 4 reveals a better agreement with the Hipparcos data for the 0.04 dex higher  $\log g$  value.

Fig. 4 also compares our analysis with the work of Oinas (1977) and Gonzalez (1998). In both cases the 0.11 dex lower iron abundance is mainly explained by the lower effective temperature, although Perrin, Cayrel & Cayrel de Strobel (1975) obtained  $[\text{Fe}/\text{H}]\sim 0.22$ , based on approximately the same low  $T_{\text{eff}}$  value. On the other hand, Campbell's (1978) analysis of near-infrared lines comes close to ours with  $T_{\text{eff}} = 5350$  K and  $[\text{Fe}/\text{H}] = +0.44$ .

Hence the existing discrepancies are mainly reduced to the value adopted for the stellar effective temperature. According to Arribas & Martínez-Roger (1989) the infrared flux method yields  $T_{\text{eff}} = 5100 \pm 150$  K, which is in favour of the lower  $T_{\text{eff}}$  value, but leads to serious discrepancies with considerations from the stellar evolutionary point of view. This is displayed in Fig. 5, where tracks with  $M_{\star} = 1.00, 1.05, 1.10$  and  $1.15 M_{\odot}$  are compared. For  $M_{\star} = 1.10 M_{\odot}$  an age less than  $\sim 1$  Gyr is implied for  $\rho^1$  Cnc, but with reference to the neighboring  $1.05 M_{\odot}$  track, higher values up to  $\sim 4$  Gyr cannot be excluded. An effective temperature as low as  $T_{\text{eff}} = 5200$  K increases this value to  $\sim 6$  Gyr, and, with the corresponding reduced metallicity, evolutionary tracks for  $[\text{Fe}/\text{H}] = +0.25$  cause an additional

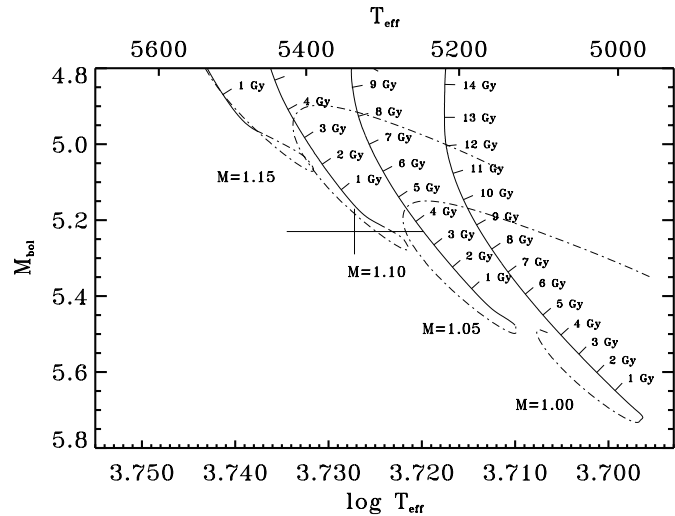


**Fig. 5.** Same as Fig. 3, but for  $\rho^1$  Cnc. The evolutionary tracks are calculated for  $M_{\star} = 1.00, 1.05, 1.10$  and  $1.15 M_{\odot}$  with  $[\text{Fe}/\text{H}] = +0.40$ . The position of  $\rho^1$  Cnc is slightly below the zero age main-sequence, which lends support to a very young object. The depicted uncertainties in  $T_{\text{eff}}$  and  $M_{\text{bol}}$ , however, also allow for an age comparable to the Solar System

shift to  $\sim 10$  Gyr. An even lower  $T_{\text{eff}} = 5100$  K yields an age above 16 Gyr. While this is of course rather unlikely, there is independent evidence in favour of an age of only 5 Gyr deduced from the mean level of the chromospheric Ca II activity by Baliunas et al. (1997). Even more, Eggen (1985) identifies  $\rho^1$  Cnc as a member of the Hyades Supercluster, young disk stars with ages probably as low as 0.3 Gyr, but unlikely beyond 2 Gyr (cf. Eggen 1992). As an upper limit to the age determination of  $\rho^1$  Cnc, we computed additional evolutionary tracks

with  $[\text{Fe}/\text{H}] = +0.33$ , our lower limit for the metallicity of the star (cf. Table 1). Even this unfavourable case does not promote values above  $\sim 5$  Gyr. An age reminiscent of old disk stars or even halo stars is therefore certainly excluded.

Baliunas et al. (1997) also report a rotational modulation of the Ca II lines of  $\rho^1$  Cnc with a mean period of  $\sim 41.7$  days. Adopting  $T_{\text{eff}}$  and  $M_{\text{bol}}$  from Table 1 the resulting stellar radius  $R_{\star} = 0.94 \pm 0.04 R_{\odot}$  implies an equatorial velocity  $v \sim 1.1 \text{ km s}^{-1}$ . This agrees with the finding of Gonzalez (1998),  $v \sin i < 1.3 \text{ km s}^{-1}$ , but is somewhat less than the  $v \sin i$  values of Baliunas et al. (1997),  $v \sin i = 1.9 \pm 1.0 \text{ km s}^{-1}$ ; Fekel (1997),  $v \sin i = 2.2 \pm 1.0 \text{ km s}^{-1}$ ; and our value,  $v \sin i = 2.5 \pm 1.0 \text{ km s}^{-1}$ .

As a final remark we note that the mass of  $\rho^1$  Cnc adopted from Fig. 5,  $M_{\star} = 1.08 M_{\odot}$ , causes the lower mass limit for the planetary companion to be  $m \sin i = 0.98 M_{\text{J}}$  (where  $M_{\text{J}}$  is the mass of Jupiter), which is slightly higher compared to the  $0.84 M_{\text{J}}$  value given in Butler et al. (1997), who assumed  $M_{\star} = 0.85 M_{\odot}$  for the primary.

### $\tau$ Bootis

Fig. 1 most evidently displays this star as the hottest member of our sample. The Balmer line wings imply an effective temperature of 6360 K, which is close to the value 6389 K derived from the infrared flux method by Blackwell & Lynas-Gray (1994). The surface gravity, if derived from the ionization equilibrium, suggests  $\log g = 3.96$ . This value gets however adjusted to  $\log g = 4.17$  from the analysis of the Mg Ib lines. Except for the few very strong lines, all absorption line profiles are notably dominated by rotational broadening (cf. Fig. 1). We derive  $v \sin i = 15.6 \pm 0.7 \text{ km s}^{-1}$ , which is rather insensitive to the exact value assumed for the macroturbulence, and close to the values found in the literature: Soderblom (1982),  $17 \pm 1 \text{ km s}^{-1}$ ; Gray (1982),  $14.8 \pm 0.3 \text{ km s}^{-1}$ ; Benz & Mayor (1984),  $14.5 \pm 0.2 \text{ km s}^{-1}$ ; Baliunas et al. (1997),  $15 \pm 1 \text{ km s}^{-1}$ ; Gonzalez (1997),  $14.5 \pm 0.5 \text{ km s}^{-1}$ ; De Medeiros, do Nascimento Jr & Mayor (1997),  $15.5 \pm 1 \text{ km s}^{-1}$ ; Fekel (1997),  $14.8 \pm 1 \text{ km s}^{-1}$ . It is only the most recent work of Wolff & Simon (1997) that shows a discrepant value,  $v \sin i = 21 \text{ km s}^{-1}$ ; their data are however intrinsically less accurate with uncertainties of at least a few  $\text{km s}^{-1}$ .

From our inferred value for the metallicity,  $[\text{Fe}/\text{H}] = +0.27 \pm 0.08$  ( $2\sigma$  rms),  $\tau$  Boo joins  $\rho^1$  Cnc as a member of the super-metal-rich stars. The corresponding  $\log T_{\text{eff}} - M_{\text{bol}}$  diagram (Fig. 6) yields an age of  $1.0 \pm 0.6$  Gyr and  $1.42 \pm 0.05 M_{\odot}$  solar masses (which again includes the uncertainty in  $[\text{Fe}/\text{H}]$ ). With a bolometric correction of  $BC_V = -0.05$  mag and with  $T_{\text{eff}}$ ,  $\log g$  and the stellar mass as derived above, the spectroscopic distance results in  $17.19 \pm 2.35$  pc. This compares with the  $15.60 \pm 0.17$  pc from the Hipparcos astrometry and – from a comparison of Fig. 7 – suggests that the stellar surface gravity may instead be  $\log g = 4.25$ , or, alternatively, the stellar mass as low as  $1.17 M_{\odot}$ . While the latter suggestion is not encouraged from inspection of Fig. 6, we cannot exclude a small systematic overestimate of the star’s metal abundance as a result

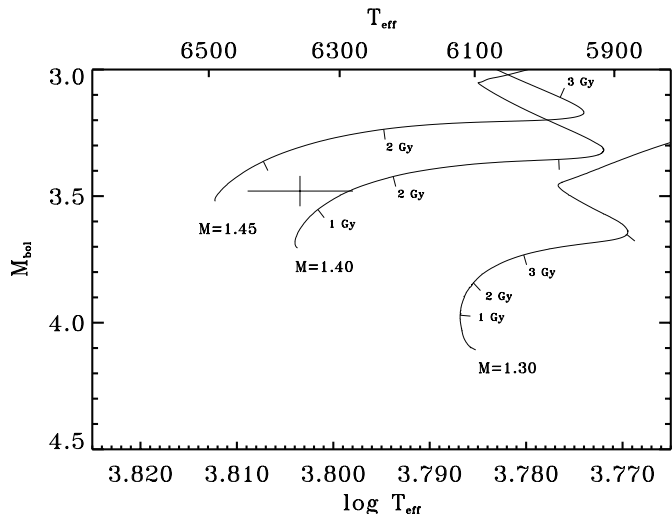


**Fig. 6.** Same as Fig. 3, but for  $\tau$  Boo. The evolutionary tracks are calculated for  $M_{\star} = 1.30, 1.40$  and  $1.45 M_{\odot}$  with  $[\text{Fe}/\text{H}] = +0.27$ . A stellar mass  $1.42 \pm 0.05 M_{\odot}$  and an age of  $1.0 \pm 0.6$  Gyr are inferred

of its comparatively high rotational velocity, that is, as a result of undetected line blends. The corresponding mass reduction is however unlikely to exceed  $0.05 M_{\odot}$ . There is also the possibility that our value for the effective temperature is erroneous, but the effect amounts to some  $\Delta T_{\text{eff}} \sim 250$  K towards lower effective temperatures (cf. Fig. 7) and aggravates the difference to the data from the infrared flux method.

If, as has been suggested by Butler et al. (1997) and Baliunas et al. (1997), the orbital and rotational periods of  $\tau$  Boo are near coincidence, the 3.31 days reported from the Doppler velocity variations imply an equatorial velocity of  $v = 22.6 \pm 0.8 \text{ km s}^{-1}$  for  $R_{\star} = 1.48 \pm 0.05 R_{\odot}$ , which is obtained from  $M_{\text{bol}} = 3.48 \pm 0.06$  and  $T_{\text{eff}} = 6360 \pm 80$  K. As a result,  $\sin i$  is confined to  $0.63 \leq \sin i \leq 0.75$ . Combining the mass function of Butler et al. (1997) and our mass estimate for the primary, the companion mass is found to be  $m \sin i = 4.35 \pm 0.11 M_{\text{J}}$ . Hence, if we assume coplanarity between the equatorial and orbital planes, the companion mass results in  $m = 6.30^{+0.78}_{-0.65} M_{\text{J}}$ , which confirms that the  $\tau$  Boo system may in fact be the large issue of 51 Peg.

### 16 Cygni A+B

Both stars are known to have properties very close to the Sun (e.g. Hardorp 1978, Neckel 1986a). Friel et al. (1993) have conducted an elaborate spectroscopic analysis of 16 Cyg A+B and we refer to this work for many additional details and references. It is only the slightly decreased surface gravities of 16 Cyg A+B which imply that both belong to the old thin-disk population, or – as Giusa Cayrel de Strobel (1996) recently wrote – we look at “... a pretty good example of what the Sun is going to be after 4 more Gyr ...”. Figs. 8 and 9 reveal that our analysis confirms the atmospheric parameters  $T_{\text{eff}}$ ,  $\log g$  and  $[\text{Fe}/\text{H}]$  of Friel et al. (1993), as well as the more recent data of Gonzalez (1998), to within the assumed error bars.

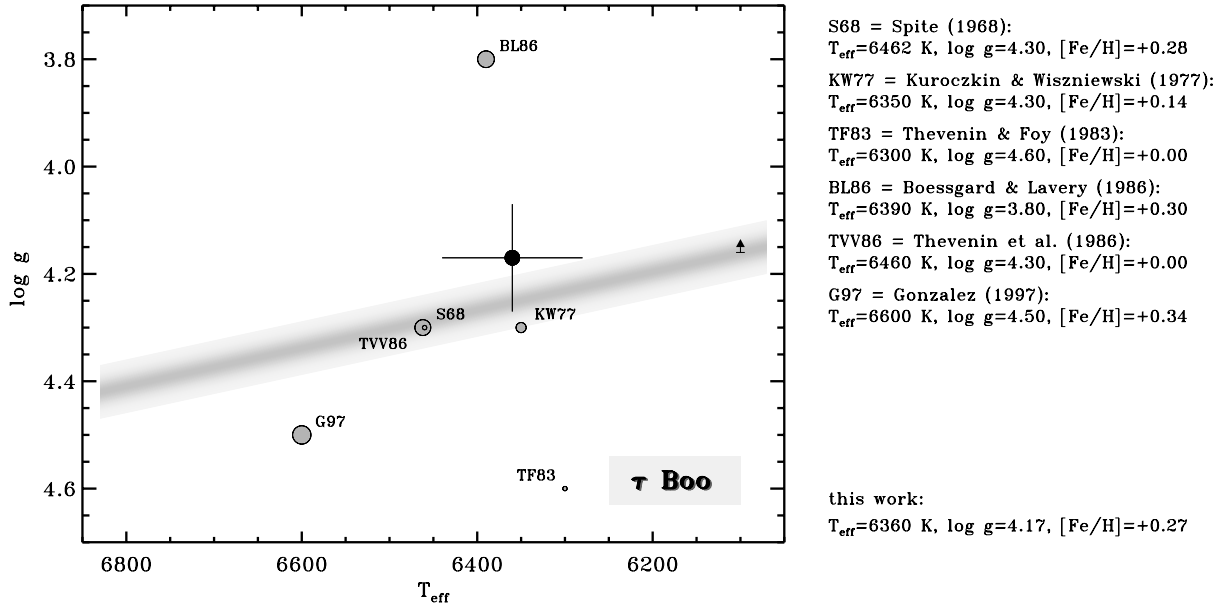


Fig. 7. Same as Fig. 2, but for  $\tau$  Boo

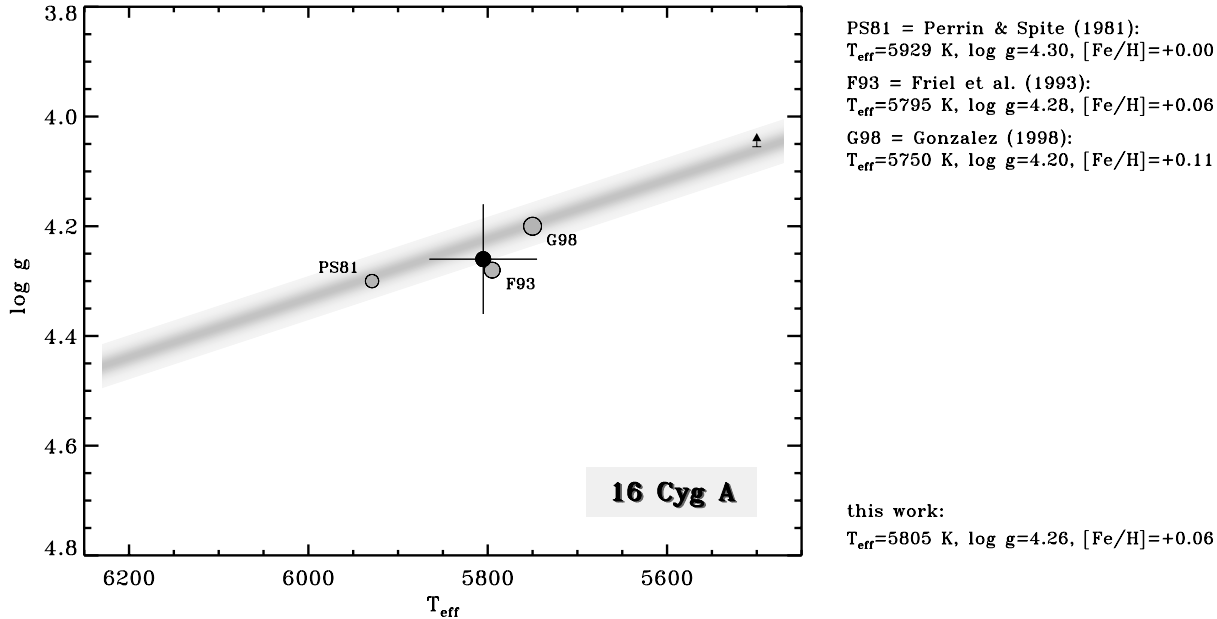


Fig. 8. Same as Fig. 2, but for 16 Cyg A

As far as the rotational velocities are concerned, we note that both stars are slow rotators, again not significantly different from the Sun, which is also confirmed by the work of Soderblom (1982), Benz & Mayor (1984) and Fekel (1997). Yet, our value for the macroturbulence parameter is merely *adopted* and this simplification prohibits any detailed comments on the exact value of  $v \sin i$ , notably the inclination angle.

Fig. 10 displays our results for the stellar masses and ages of 16 Cyg A+B. Both stars reveal an almost identical metal content and are therefore compared in the same diagram. 16 Cyg A, being the slightly hotter object, is accordingly more evolved in  $M_{\text{bol}}$ . The tick marks of the evolutionary tracks with  $[\text{Fe}/\text{H}] =$

+0.05 imply a common age of  $\sim 8.0$  Gyr, which is accurate to 1.4 Gyr for 16 Cyg A, and 1.8 Gyr for 16 Cyg B, if we take uncertainties of  $\Delta T_{\text{eff}} = 60$  K,  $\Delta M_{\text{bol}} = 0.06$  mag and  $\Delta[\text{Fe}/\text{H}] = 0.05$  dex into account. The stellar masses are found to be  $M_A = 1.04 \pm 0.04 M_{\odot}$  and  $M_B = 1.01 \pm 0.04 M_{\odot}$  for the A and B component, respectively. This again agrees very well with the findings of Friel et al. (1993),  $M_A = 1.05 \pm 0.05 M_{\odot}$  and  $M_B = 1.00 \pm 0.05 M_{\odot}$ , as well as Gonzalez (1998),  $M_A = 1.00 \pm 0.03 M_{\odot}$  and  $M_B = 0.97 \pm 0.03 M_{\odot}$ . As a result of the well-defined bolometric magnitudes, as well as our good knowledge of the effective temperatures, quite accurate stellar radii can be derived:  $R_A = 1.29 \pm 0.04 R_{\odot}$  for 16 Cyg A, and

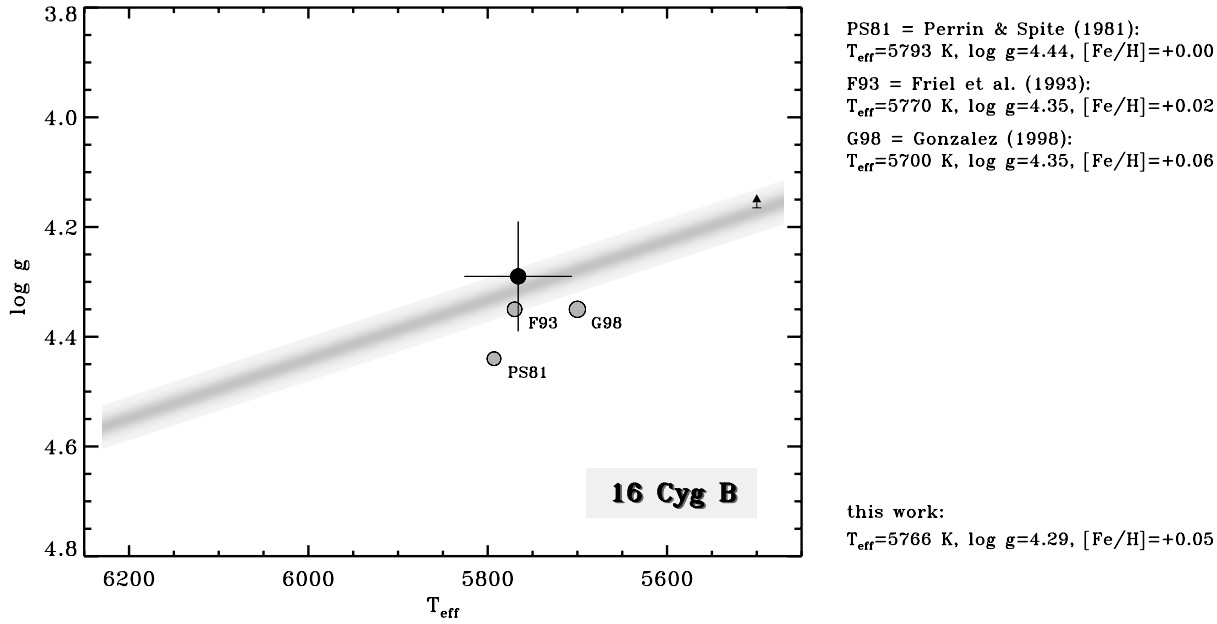


Fig. 9. Same as Fig. 2, but for 16 Cyg B

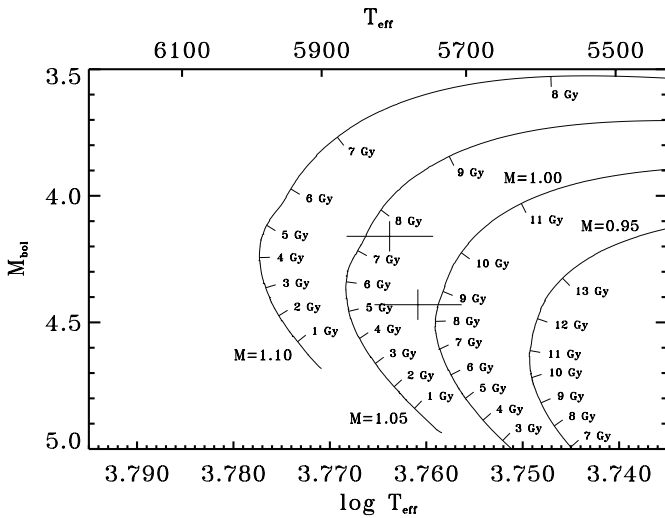


Fig. 10. Same as Fig. 3, but for 16 Cyg A+B. The evolutionary tracks are calculated for  $M_{\star} = 0.95, 1.00, 1.05$  and  $1.10 M_{\odot}$  with  $[\text{Fe}/\text{H}]=+0.05$ . Stellar masses and ages are found to be  $1.04 \pm 0.04 M_{\odot}$  and  $8.0 \pm 1.4$  Gyr for 16 Cyg A, and  $1.01 \pm 0.04 M_{\odot}$  and  $8.0 \pm 1.8$  Gyr for 16 Cyg B

$R_B = 1.16 \pm 0.04 R_{\odot}$  for 16 Cyg B, i.e. in both cases the error is less than 4%. We note that these values are almost identical to those of the older work of Neckel (1986b),  $R_A \approx 1.25 \pm 0.03 R_{\odot}$  and  $R_B \approx 1.15 \pm 0.05 R_{\odot}$ . He derived upper limits for the luminosity of the stars, which resulted in a maximum distance of  $\sim 22$  pc, significantly lower than all trigonometric-parallax-based distances available at that time, but in excellent agreement with the Hipparcos data.

### $\rho$ Coronae Borealis

The model atmosphere analysis of this star is somewhat more complicated, since  $\rho$  CrB is depleted in metals by a factor of two, but at the same time also enriched in the  $\alpha$ -element magnesium by  $[\text{Mg}/\text{Fe}]=+0.19$ . Thus, the modeling was performed on both of our grids of model atmospheres, one with a solar mixture of relative abundances (hereafter referred to as “ $\odot$ ”), the other with  $\alpha$ -elements (O, Ne, Mg, Si, S, Ar, Ca and Ti) enhanced by +0.4 dex, which is close to the element mixture found in many metal-poor halo stars.

For the  $\odot$ -modeling the Balmer line wings of  $\text{H}\alpha$  and  $\text{H}\beta$  result in  $T_{\text{eff}} = 5795$  K and the ionization equilibrium yields  $\log g = 4.18$  and  $[\text{Fe}/\text{H}] = -0.26$ . This surface gravity value, however, leads to discrepancies with the Mg Ib lines and requires a *downward* revision to  $\log g = 4.05$ . The metallicity – now based on only Fe II lines – is found to be  $[\text{Fe II}/\text{H}] = -0.32$ . On the other hand, modeling by means of the grid of atmospheres with enhanced  $\alpha$ -elements results in  $T_{\text{eff}} = 5847$  K,  $\log g = 4.06$  and  $[\text{Fe}/\text{H}] = -0.26$ . Contrary to the  $\odot$ -modeling, the wings of the Mg Ib lines now support a *higher* value for the surface gravity,  $\log g = 4.19$ , which entails  $[\text{Fe II}/\text{H}] = -0.16$ . Interpolation within both sets of parameters leads to  $T_{\text{eff}} = 5821$  K,  $\log g = 4.12$  and  $[\text{Fe}/\text{H}] = -0.24$ . Estimated errors are  $\Delta T_{\text{eff}} = 80$  K,  $\Delta \log g = 0.1$  dex and  $\Delta[\text{Fe}/\text{H}] = 0.08$  dex.

Fig. 11 compares our model atmosphere analysis of  $\rho$  CrB with other investigations reported in the literature. We also mention the recent effective temperature determinations of Gray (1994),  $T_{\text{eff}} = 5868$  K, and Alonso, Arribas & Martínez-Roger (1996),  $T_{\text{eff}} = 5777$  K, which are based on spectral line-depth ratios and the infrared flux method, respectively. All these data consistently support a metal-poor, slightly evolved star of approximately solar effective temperature. With  $T_{\text{eff}} =$

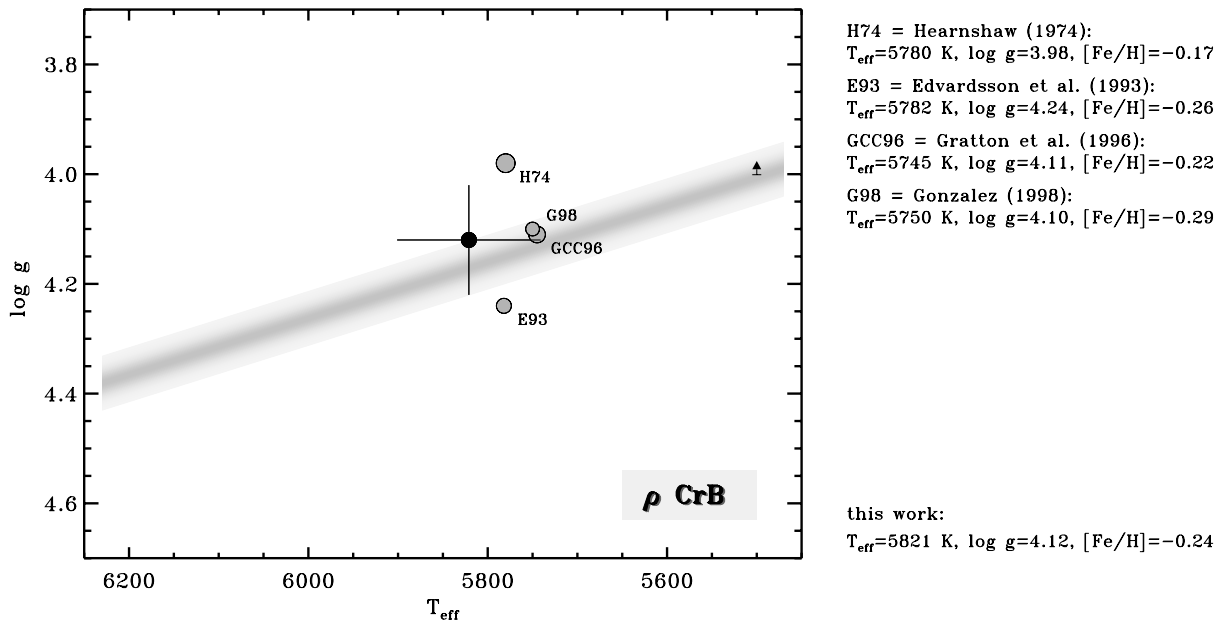


Fig. 11. Same as Fig. 2, but for  $\rho$  CrB

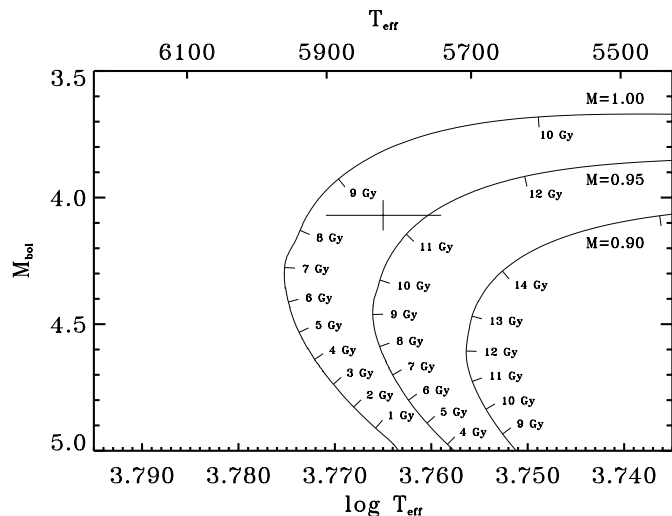


Fig. 12. Same as Fig. 3, but for  $\rho$  CrB. The evolutionary tracks are calculated for  $M_{\star} = 0.90, 0.95$  and  $1.00 M_{\odot}$  with  $[\text{Fe}/\text{H}] = -0.24$ . The stellar mass and age inferred are,  $0.97 \pm 0.05 M_{\odot}$  and  $10.2 \pm 1.7$  Gyr, respectively

$5821 \pm 80$  K and  $M_{\text{bol}} = 4.07 \pm 0.06$  we obtain a stellar radius  $R_{\star} = 1.34 \pm 0.05 R_{\odot}$ , which also establishes the evolved stage of  $\rho$  CrB. According to the evolutionary tracks in Fig. 12 the star has already reached its turnoff region, thereby an age of  $10.2 \pm 1.7$  Gyr is deduced along with a mass of  $M_{\star} = 0.97 \pm 0.05 M_{\odot}$ . As a cautionary remark we note however that our displayed tracks of  $\rho$  CrB have not been calculated with  $\alpha$ -enhanced opacities.

From their Ca II activity-rotation relation Noyes et al. (1984) compute a rotational period  $P_{\text{calc}} = 19.7$  days for  $\rho$  CrB. According to Baliunas, Sokoloff & Soon (1996) there is also observational evidence of fluctuations in the Ca II flux with a period

of  $P_{\text{obs}} = 17$  days, although that evidence is considered to be marginal (cf. Noyes et al. 1997, p.112). Both values lead to equatorial velocities  $v = 3.4$  km s $^{-1}$  and  $v = 4.0$  km s $^{-1}$ , respectively. Combined with the published projected rotational velocities of Soderblom (1982),  $v \sin i = 1.5 \pm 0.5$  km s $^{-1}$ ; Benz & Mayor (1984),  $v \sin i = 1.2 \pm 0.7$  km s $^{-1}$ ; Gonzalez (1998),  $v \sin i \sim 1.5$  km s $^{-1}$ ; and our value  $v \sin i = 1.0 \pm 1.0$  km s $^{-1}$ , this implies a rather low stellar inclination ( $i \leq 35^{\circ}$ ), that renders observable planetary transits unlikely, at variance with the results of Hale & Doyle (1994) who favour  $i \sim 90^{\circ}$ .

#### 4. Discussion

In the preceding section we have presented the results from model atmosphere analyses and evolutionary calculations of six nearby stars, which have met considerable attention since the announcement of massive planetary companions around them. Along with 51 Peg and 47 UMa, which are also deemed to possess orbiting planets, we may address here a few aspects of this increasing sample of stars.

One major characteristic that is also discussed in the literature (Gonzalez 1997, 1998, Butler et al. 1997, Marcy et al. 1997, Laughlin & Adams 1997) is the amount of metals found in the stellar abundance analyses. No doubt, 51 Peg,  $\tau$  Boo and especially  $\rho^1$  Cnc belong to the group of super-metal-rich stars and it may well be that a large provision of heavy elements is conducive to mechanisms of planet formation in the precursor disk environment. Even more, the unexpected tight orbits of the majority of the detected planets are suggestive of contamination scenarios, whereby a gradually inwards migrating giant planet sweeps most of the intervening disk material onto the stellar surface. But with the sample of extrasolar systems enlarged by the late-comers  $\rho$  CrB and 16 Cyg A+B, there is now solid information that, first,  $\rho$  CrB is an example of a star with sub-

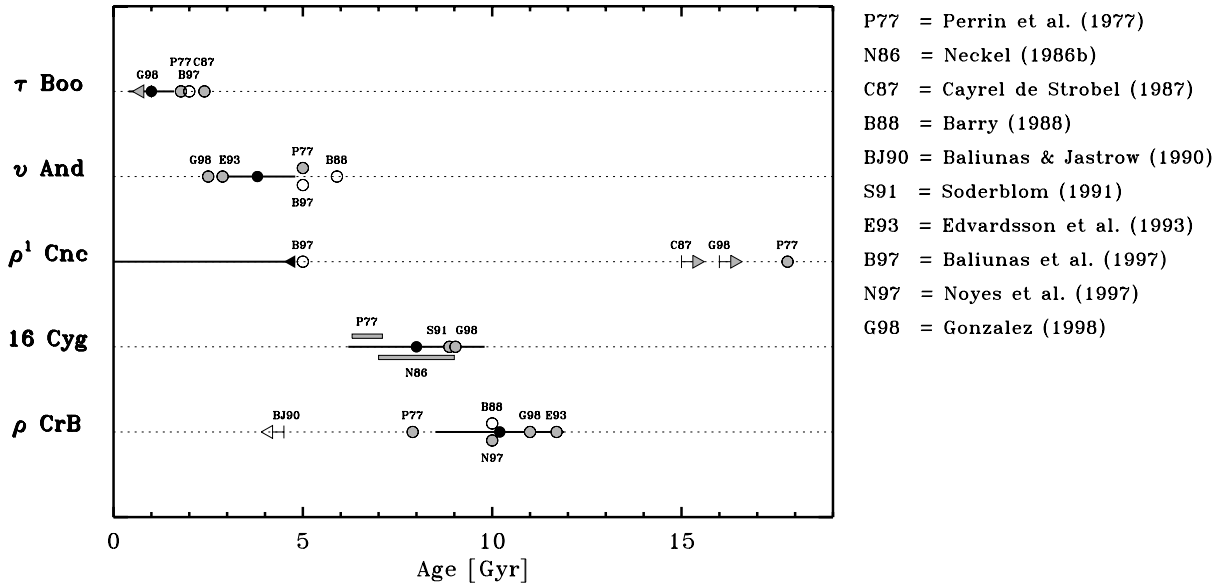


Fig. 13. Age determinations (black symbols) of the planetary candidate stars, compared to literature data from isochrone fitting (grayscale symbols) and activity-age or rotation-age relations (open symbols)

solar metallicity and, second, the common iron abundance of 16 Cyg A and B does not promote the self-enrichment scenario.

The other stars, 47 Uma and  $\nu$  And, as well as 16 Cyg A and B, reveal a close to solar metal abundance. Recent observational evidence however suggests (e.g. Wyse & Gilmore 1995, Rocha-Pinto & Maciel 1996) that even this value exceeds the maximum found for the local metallicity distribution function by  $\sim 0.2$  dex. In this case, all stars, except for  $\rho$  CrB, may be considered as “metal-rich” objects. Yet, many abundance studies, in particular those that deal with large samples, employ photometric metallicity calibrations that can easily be misleading for the more metal-rich stars:  $\nu$  And and  $\rho^1$  Cnc are only two examples, that show a considerable spread of values in the literature. Therefore, we consider it premature to put too much weight to the observed metal abundances of the planetary system candidate stars.

Another aspect that has to be mentioned is the uncertainty of stellar age determinations, which we display in Fig. 13 for the individual stars. Notably the age information can provide valuable constraints on e.g. the efficiency of tidal interactions for orbital synchronization and circularization, as well as the more general question, whether stellar pulsations are conceivable alternatives to the observed reflex motions. With the availability of the accurate Hipparcos data and the improved stellar evolutionary calculations of Bernkopf (1998), which are now also revised to allow for the effects of helium diffusion, we consider the stellar ages summarized in Table 1 to be indeed at a high confidence level. It is only the above mentioned self-pollution scenario that may alter the chemical composition of the outer stellar layers and then acts as a mask for a correct interpretation of the stellar spectra.

Finally, we comment on the results of the *spectroscopically* determined stellar surface gravities. We recall that  $\rho^1$  Cnc, being significantly cooler than the Sun, attains very similar values

from either the strong Mg Ib line method or the iron ionization equilibrium. On the other hand, a clear distinction is found for the hotter objects,  $\nu$  And and  $\tau$  Boo, where the Hipparcos parallaxes reveal systematic discrepancies if we make use of the LTE iron ionization equilibria in combination with our model atmospheres. As a result, and keeping in mind that our sample stars are very nearby, the lesson from the solid astrometric data is that the  $\log g$ 's are in fact reliable to 0.1 dex for dwarfs and slightly evolved stars of similar spectral types, as long as we stick closely to the diagnostics stored in the wings of the Mg Ib lines.

*Acknowledgements.* J.B. acknowledges support of this research from the *Deutsche Forschungsgemeinschaft, DFG* under Be 2015/1-2 and Ge 490/12-2. K.F. is grateful for two travel grants under Fu 198/2-1 + Fu 198/4-1 and financial support from the *BMBF* under grant 05 2MU114 7. We thank G. Gonzalez for useful discussions and for sending us his results in advance of publication. This research has made use of the SIMBAD database, operated at CDS, Strasbourg, France.

## References

- Alonso, A., Arribas, S., Martínez-Roger, C., 1995, A&A 297, 197
- Alonso, A., Arribas, S., Martínez-Roger, C., 1996, A&AS 117, 227
- Arribas, S., Martínez-Roger, C., 1989, A&A 215, 305
- Balachandran, S., 1990, ApJ 354, 310
- Baliunas, S., Jastrow, R., 1990, Nat 348, 520
- Baliunas, S.L., Sokoloff, D., Soon, W., 1996, ApJ 457, L99
- Baliunas, S.L., et al., 1997, ApJ 474, L119
- Barry, D.C., 1988, ApJ 334, 436
- Benz, W., Mayor, M., 1984, A&A 138, 183
- Bernkopf, J., 1998, A&A 332, 127
- Blackwell, D.E., Lynas-Gray, A.E., 1994, A&A 282, 899
- Boesgaard, A.M., Lavery, R.J., 1986, ApJ 309, 762
- Butler, R.P., et al., 1997, ApJ 474, L115
- Campbell, B., 1978, AJ 83, 1430

- Carney, B.W., 1979, ApJ 233, 211  
Cayrel de Strobel, G., 1987, JApA 8, 141  
Cayrel de Strobel, G., 1996, A&AR 7, 243  
Cayrel de Strobel, G., et al., 1997, A&AS 124, 299  
Cochran, W.D., et al., 1996, BAAS 28, 1111  
Cochran, W.D., et al., 1997, ApJ 483, 457  
De Medeiros, J.R., do Nascimento Jr, J.D., Mayor, M., 1997, A&A 317, 701  
Edvardsson, B., et al., 1993, A&A 275, 101  
Eggen, O.J., 1985, AJ 90, 74  
Eggen, O.J., 1992, AJ 104, 1482  
Fekel, F.C., 1997, PASP 109, 514  
Friel, E., et al., 1993, A&A 274, 825  
Fuhrmann, K., Pfeiffer, M.J., Bernkopf, J., 1997, A&A 326, 1081  
Gonzalez, G., 1997, MNRAS 285, 403  
Gonzalez, G., 1998, A&A 334, 221  
Gratton, R.G., Carretta, E., Castelli, F., 1996, A&A 314, 191  
Gray, D.F., 1982, ApJ 258, 201  
Gray, D.F., 1984, ApJ 281, 719  
Gray, D.F., 1986, PASP 98, 319  
Gray, D.F., 1992, *The observation and analysis of stellar photospheres*, Cambridge Univ. Press  
Gray, D.F., 1994, PASP 106, 1248  
Hale, A., Doyle, L.R., 1994, Ap&SS 212, 335  
Hardorp, J., 1978, A&A 63, 383  
Hearnshaw, J.B., 1974, A&A 36, 191  
Kuroczkin, D., Wiszniewski, A., 1977, Acta Astron. 27, 145  
Kurucz, R.L., Furenlid, I., Brault, J., Testerman, L., 1984, *Solar Flux Atlas from 296 to 1300 nm*, KPNO, Tucson  
Laughlin, G., Adams, F.C., 1997, ApJ 491, L51  
Marcy, G.W., et al., 1997, ApJ 481, 926  
Mermilliod, J.-C., Mermilliod, M., Hauck, B., 1997, A&AS 124, 349  
Neckel, H., 1986a, A&A 159, 175  
Neckel, H., 1986b, A&A 167, 97  
Noyes, R.W., et al., 1984, ApJ 279, 763  
Noyes, R.W., et al., 1997, ApJ 483, L111  
Oinas, V., 1977, A&A 61, 17  
Perrin, M.-N., Spite, M., 1981, A&A 94, 207  
Perrin, M.-N., Cayrel, R., Cayrel de Strobel, G., 1975, A&A 39, 97  
Perrin, M.-N., et al., 1977, A&A 54, 779  
Powell, A.L.T., 1970, MNRAS 148, 477  
Pfeiffer, M.J., et al., 1998, A&A 130, 381  
Rocha-Pinto, H.J., Maciel, W.J., 1996, MNRAS 279, 447  
Saxner, M., Hammarbäck, G., 1985, A&A 151, 372  
Soderblom, D.R., 1982, ApJ 263, 239  
Soderblom, D.R., 1985, AJ 90, 2103  
Soderblom, D.R., 1991, ApJ 375, 722  
Spite, M., 1968, Ann. Astron. 31, 269  
Spite, M., Spite, F., 1973, A&A 23, 63  
Thévenin, F., Foy, R., 1983, A&A 122, 261  
Thévenin, F., Vauclair, S., Vauclair, G., 1986, A&A 166, 216  
Tomkin, J., et al., 1997, A&A 327, 587  
VandenBerg, D.A., Bell, R.A., 1985, ApJS 58, 561  
Wyse, R.F.G., Gilmore, G., 1995, AJ 110, 2771  
Wolff, S.C., Simon, T., 1997, PASP 109, 759